

# Some Theoretical and Practical Perspectives of the Travel Time Kinematic Wave Model: Generalized Solution, Applications, and Limitations

Peter J. Jin<sup>a\*</sup> Ke Han<sup>b†</sup> Bin Ran<sup>c‡</sup>

<sup>a</sup>*Department of Civil, Architectural, and Environmental Engineering  
University of Texas at Austin, Austin, TX 78701, USA*

<sup>b</sup>*Department of Mathematics  
Pennsylvania State University, University Park, PA 16802, USA*

<sup>c</sup>*Department of Civil and Environmental Engineering  
University of Wisconsin-Madison, Madison, WI 53706, USA*

Submitted for presentation at the 93<sup>rd</sup> Annual Meeting of Transportation Research Board,  
January, 2014

Word count based on Latex: 5328 words + 7 figures + 1 table = 7328

## Abstract

This paper explores the travel time kinematic wave (KW) model recently-revealed through Hamilton-Jacobi (H-J) Partial Differential Equation (PDE) theory proposed by Laval and Leclercq. We focus on theoretical and practical aspects of the travel time KW model in real-world traveler information and traffic management applications. The travel time kinematic wave (KW) model is an equivalent representation of the Lighthill-Whitham-Richards (LWR) model. The model preserves both the spatial representation in Euler model and the numerical and formulation benefits in Lagrangian model, making it suitable for conducting traffic state estimation based on prevailing mobile sensor data such as GPS, cellular, and Bluetooth probe data. In this paper, we provide an in-depth discussion on the physical meaning of the model revealed through a heuristic derivation of the travel time KW model and the rigorous proof of its equivalence to the other two Euler and Lagrangian models. We extend the Lax-Hopf formulations and solution methods proposed in Laval and Leclercq's study to account for internal boundary problems that may be used to formulating signalized intersection, active traffic management, and the emerging connected vehicle data. Meanwhile, by comparing the two Lagrangian formulations of LWR with respect to vehicle sinks and sources, route-based, and lane-based applications, we attempt to provide a realistic perspective on the potentials and challenges facing Lagrangian traffic flow models.

**Keywords:** macroscopic traffic flow model, Lagrangian coordinate, probe vehicle technologies

---

\*Corresponding author, Tel: +1 512-232-3124. E-mail address: jjin@austin.utexas.edu

†E-mail: kxh323@gmail.com

‡E-mail: bran@engr.wisc.edu

# 1 Notations

$n$ : number of vehicles, the order of a vehicle after a reference vehicle, Lagrangian coordinate.

$x$ : location, distance on a road.

$t$ : time, duration.

$k$ : density,  $k = -n_x$  (where  $n_x$  represents the partial derivative of  $n$  over  $x$ )

$q$ : flow,  $q = n_t$

$u$ : speed,  $u = x_t$

$h$ : distance headway between two vehicles,  $h = -x_n$ ,  $h = 1/k$ .

$\tau$ : travel time density, travel time over a unit distance,  $\tau = t_x$ , and  $\tau = 1/u$ .

$p$ : time headway between two vehicles,  $p = t_n$  and  $p = 1/q$ .

# 2 Introduction

The first-order vehicular conservation model (LWR model) proposed by Lighthill and Whitham (1955) and Richards (1956) has been the foundation of the continuum traffic flow theory. It is the most widely-used macroscopic traffic flow model, particularly after Daganzo's seminal work on the cell transmission model that solves the LWR model efficiently at large scales. One key benefit of LWR model is that traffic data from traditional fixed-location detectors (e.g. loop detectors) can be efficiently plugged into the model for traffic state estimation and prediction. Over the last decade, the probe vehicle technologies such as GPS, cellphone, and Bluetooth probe vehicle technologies have experienced rapid development and deployment and become a key data source in traveler information provision. Traffic data collected from mobile sensor technologies have different characteristics than the fixed-location sensor data. The data is usually collected with individual vehicles rather than at fixed-location at fixed time intervals. The data usually relies on complicated data processing techniques to fix the space-time models which can lead to unreliable estimation results especially with sampling error and data noises. Under such background, Lagrangian coordinate based traffic flow models start to attract the attention of both traffic flow theorists and modelers. The Lagrangian coordinate was first introduced into traffic flow from hydrodynamics by Moskowitz (1965) and elaborated by Makigami et al. (1971). In hydrodynamics, the Lagrangian coordinate is defined as the following.

$$n(x, t) = - \int_{x(t)}^x k(s, t) ds \quad (2.1)$$

The equivalent traffic flow definition is found to be the order of vehicles with preceding vehicles always have smaller Lagrangian coordinate than following vehicles. It should be noted that this coordinate does not stick to a physical vehicle. In multi-lane situation when vehicle passes one another their vehicle orders will switch.

Figure 1 illustrates the physical meaning of Lagrangian coordinate. In the vehicular coordinate, the origin can be a selected reference vehicle and the coordinate does not stick with physical vehicles. When one vehicle passing the other vehicle in a multi-lane segment, their vehicular coordinates switches as illustrated with the yellow and green vehicles. The vehicular coordinate, in the form of accumulative vehicles at a cross section, has been widely used in studying traffic flow characteristics and highway capacity (Banks, 1990, 1991; Cassidy and Bertini, 1999; Cassidy and Windover, 1995). The concept also leads to the development of the Variational Theory for traffic flow first proposed by Luke (1972) and Newell (1993a, b, c), and completed by Daganzo (2005a, b).

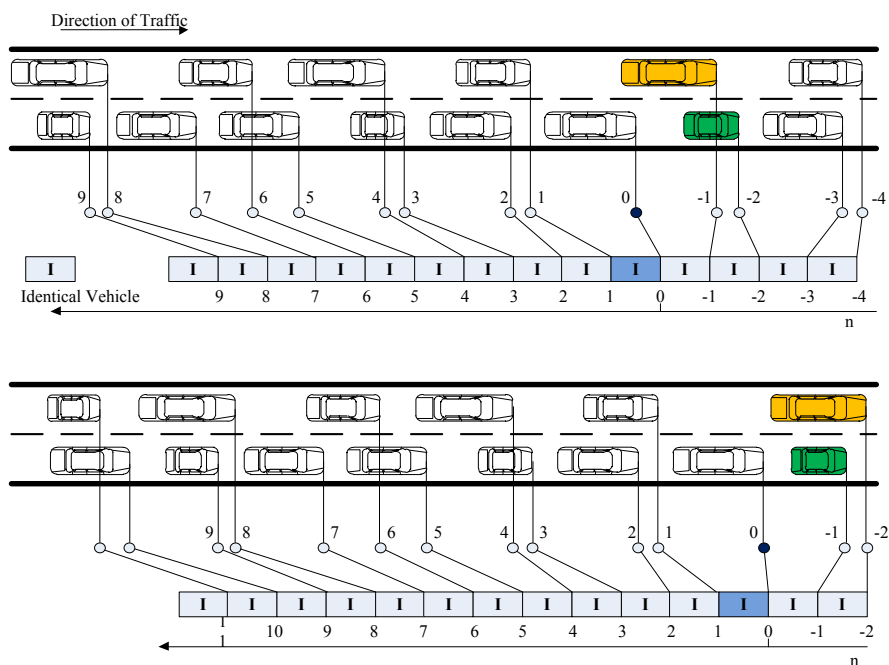


Figure 1: Illustration of the Lagrangian Coordinate. Notice that the coordinates are changed when the yellow vehicle overtakes the green vehicle.

Lagrangian coordinate can be incorporated into the continuum traffic flow modelling in two different ways. The first one is to establish moving boundary conditions for the Euler formulations using measurements over the Lagrangian coordinate (Claudel and Bayen, 2010a, b; Herrera and Bayen, 2010). The other one is to use the Lagrangian coordinate similar to the Lagrangian formulation in the hydrodynamics. Leclercq et al. (2007) first studied the hydrodynamic Lagrangian model under the context of traffic flow theory. It is found that the Lagrangian model with respect to vehicle and time can be derived by using a space function based variational theory. The model exhibits some significant numerical advantages over the original space-time model for problems with respect to moving coordinates, e.g. moving bottlenecks. Furthermore, the solution of Godunov scheme converges to an upwind scheme under a triangular fundamental diagram for the Lagrangian formulation. Lagrangian coordinate can also be used to reformulate multi-class models (van Wageningen-Kessels et al., 2010), network models (van Wageningen-Kessels et al., 2013), and high-order traffic flow models such as Aw-Rascle models (Moutari and Rascle, 2007).

The travel time kinematic wave (KW) model is revealed by the Hamilton-Jacobi theory recently proposed by Laval and Leclercq (2013). By defining a traffic flow surface with respect to three two-dimensional coordinate systems, the HJ formulation can be applied to derive the existing Euler (LWR Model) and Lagrangian-time model, as well as the Lagrangian-space Travel Time KW model. The paper further derive the Lax-Hopf boundary formulations for piece-wise linear empirical support and rectangular boundary problems. With the theoretical foundation profoundly established by Laval and Leclercq (2013)'s work, this paper attempts to investigate the practical perspectives regarding the physical meaning of the new model, its relationship to the other two models, and the model implementation in real-world traveler information and traffic management applications. We identified and proposed a Lax-Hopf

framework for the missing irregular boundary problem formulations so that the model can be used in practice to model signalized intersection, freeway control strategies, and the emerging connected vehicle data sources. We discussed the limitations of the model with respect to vehicle sinks and sources and in lane-based applications.

### 3 Physical Aspects of The Travel Time Kinematic Wave (KW) Model

#### 3.1 The heuristic derivation of the travel time KW model

The travel time KW model can be derived by considering a single-lane road section with two paired vehicle tracking stations that can measure the vehicle travel times on the road section. The two detectors are located at  $x$  and  $x + \Delta x$  as shown in Figure 2. We investigate two consecutive groups of  $\Delta n$  vehicles with their leading vehicles being  $n$ th and  $(n + \Delta n)$ th vehicle in the traffic stream respectively. The total travel time for each vehicle group to pass through the road section are  $t$  and  $t + \Delta t$  respectively. The temporal headway changes from  $p$  in the first group to  $p + \Delta p$  in the second group, then  $\Delta t$  can be written as

$$\Delta t = (p + \Delta p) \Delta n - p \Delta n = \Delta p \Delta n \quad (3.2)$$

If we define the travel time ratio  $\tau$  as the inverse of the space mean speed of a vehicle group,  $\Delta t$  can also be interpreted as the changes of the travel time ratio on the segment. The travel time ratio is assumed to be  $\tau$  when the first vehicle group starts to exit the section; while it changes to  $\tau + \Delta \tau$  when the second vehicle group starts to exit, then  $\Delta t$  can also be calculated as the following.

$$\Delta t = (\tau + \Delta \tau) \Delta x - \tau \Delta x = \Delta \tau \Delta x \quad (3.3)$$

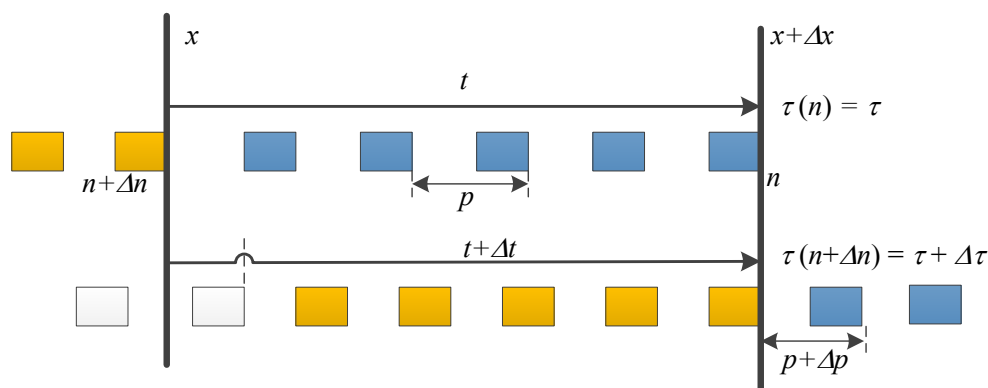


Figure 2: Physical Derivation of the Travel Time KW Model

Since Equations (3.2) and (3.3) describe the same quantity, we have

$$\Delta t = \Delta p \Delta n = \Delta \tau \Delta x. \quad (3.4)$$

Thus, the differencing formulation can be obtained for the travel time KW model as the following

$$\frac{\Delta p}{\Delta x} - \frac{\Delta \tau}{\Delta n} = 0 \quad (3.5)$$

Considering all the medium are continuous including vehicle numbers and allowing the increment to be infinitesimal, it follows that

$$\tau_n - p_x = 0 \quad (3.6)$$

This section mainly focuses on interpreting the physical meaning of the travel time KW model. More rigorous derivation based on variational theory and Hamilton-Jacobi theory can be found in Laval and Leclercq (2013).

### 3.2 Godunov Numerical Scheme

The proposed model is a typical nonlinear first-order hyperbolic conservation equation. Its solution can be obtained by the characteristic method and the Rankine–Hugoniot condition. The slope of the shock boundary between two states  $(p_1, \tau_1)$  and  $(p_2, \tau_2)$  in the n-x diagram can be obtained as the following.

$$s_{nx} = -\frac{p_1 - p_2}{\tau_1 - \tau_2} = \frac{p_2 - p_1}{\tau_1 - \tau_2} \quad (3.7)$$

In the travel time KW model, the slope of the shock wave boundary means the changing rate of the shock boundary caused by each unit vehicle switching between the vehicle groups at both sides of the shock. Meanwhile, the solutions from the proposed model are equivalent to the corresponding LWR and Lagrangian model even with source term and in weak sense. Godunov scheme can be used to solve the travel time KW model efficiently. Considering a numerical grid with a resolution of  $\Delta n$  and  $\Delta x$  for Lagrangian and space coordinate respectively. Then the Godunov scheme can be written as the following.

$$T_x^{n+\Delta n} = T_x^n + \frac{\Delta n}{\Delta x} [p(T_x^n, T_{x+\Delta x}^n) - p(T_{x-\Delta x}^n, T_x^n)] \quad (3.8)$$

where  $T_x^n$  denotes the average  $\tau$  values obtained for the grid at  $(n, x)$ ,  $p$  is a function to be obtained when solving the Riemann problem (See the Godunov Procedure listed at the end of this section), given the travel time ratio experienced by the previous vehicle group on the road section  $x$  and its downstream section at  $(x+\Delta x)$ . Meanwhile, the CFL (Courant-Friedrichs-Lewy) condition (Courant et al., 1967) for the travel time KW model over the rectangle grids on the n-x diagram is as the following.

$$\left| \frac{\Delta n}{\Delta x} \right| \leq \left| \frac{1}{p'(\tau)} \right| \quad (3.9)$$

The above CFL condition can be implemented in two ways. When fixing the size of the vehicle group which can be constrained by the sampling rate of a particular vehicle detection technologies, we divided road segments equivalent to its maximal characteristic spacing (e.g. free flow spacing), that is,

$$\Delta x \geq |p'(\tau)|_{max} \Delta n \quad (3.10)$$

The other way is to fix the segment length required by ATIS (Advanced Traveler Information System) applications, then the CFL condition can be used to determine the number of vehicles  $\Delta n$  to be processed at each numerical iteration.

$$\Delta n \leq \frac{\Delta x}{|p'(\tau)|_{max}} \quad (3.11)$$

The fixed  $\Delta n$  method can ensure the estimation accuracy but it can lead to large  $\Delta x$  that are meaningless for ATIS applications. Even though the sample size may not be sufficient to support traffic state estimation at every segment, the fixed  $\Delta x$  method are more flexible for 1) tuning the resolution of the Lagrangian coordinate and 2) the implementation of pre-defined ATIS reporting spatial resolutions. Furthermore, by fixing the segment length, the numerical method can incorporate the segment based representation used in numerical methods for LWR model while still allowing flexibility in adjusting the resolution of the solutions on the Lagrangian coordinate.

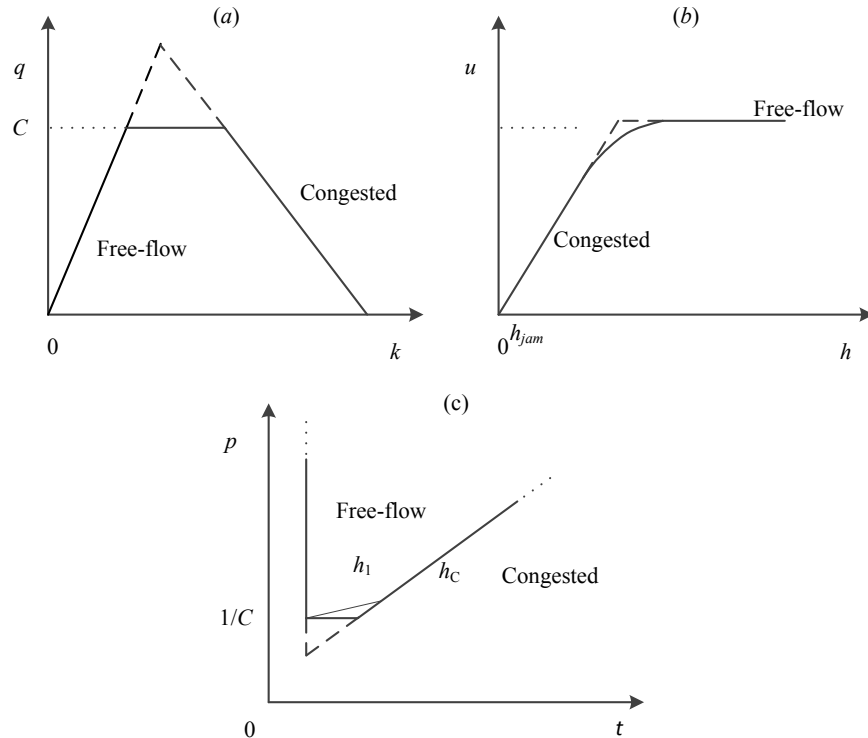


Figure 3: Triangular  $q-k$  and  $p-\tau$  diagram, Shock waves in  $n-x$  diagram

In Daganzo's cell transmission model (Daganzo, 1994), the triangular flow-density relationship is introduced to reduce the infinitely many directions of characteristics with continuous FDs to only two or three directions depending on the capacity constraint. It substantially reduces the complexity of the Godunov scheme which leads to highly-efficient numerical methods. Triangular FD can also simplify the Godunov scheme for the travel time kinematic wave model. Figure 3 (a,b) compares the geometric characteristics between the triangular  $q-k$  and  $p-\tau$  diagram. In triangular FDs, the free-flow regime only has one uniform speed which corresponds to a vertical line on the  $p-\tau$  diagram; while the congested regime in  $p-\tau$  diagram is linear. If a capacity constraint is added, the  $p-\tau$  diagram is then cut-off at the bottom creating a saturated regime with time headway of  $1/C$  (where  $C$  is the capacity). In the following, the Godunov based numerical methods for the proposed travel time KW model are summarized.

**Numerical Grid:** The entire road section is divided into  $M$  segments with a width of  $\Delta x$  and each segment is denoted by  $m$ . Using CFL condition in Equation (3.10), the total amount of vehicles to be investigated are divided into  $I$  vehicle groups.

**Initial condition:** Travel time ratio  $\tau_m^0$  on each segment  $i$  experienced by vehicle group  $m = 0$ .

**Boundary condition:** Time headway  $p_0^i$  and  $p_M^i$  of each vehicle group  $i$  when entering the first link  $m = 1$  and exiting the last link  $m = M$ .

**Numerical Methods:**

For  $i = 1 : I$

For  $m = 1 : M$

$$T_m^i = T_m^{i-1} + \frac{\Delta n}{\Delta x} [p(T_m^{i-1}, T_{m+1}^{i-1}) - p(T_{m-1}^{i-1}, T_m^{i-1})] \quad (3.12)$$

where

$$p(\tau_l, \tau_r) = \begin{cases} \min_{\tau_l \tau \tau_r} p(\tau), & \text{if } \tau_l \leq \tau_r \\ \max_{\tau_r \tau \tau_l} p(\tau), & \text{if } \tau_l > \tau_r \end{cases} \quad (3.13)$$

End

End

## 4 Equivalence Between Eulerian and Lagrangian Formulations

In this section, we provide rigorous mathematical analysis on the equivalence between the Hamilton-Jacobi equation for  $T(n, x)$

$$T_n - P(T_x) = 0 \quad (4.14)$$

which is the integral form of (3.6), and the H-J equation in the Lagrangian coordinate for  $X(n, t)$

$$X_t - V(-X_n) = 0 \quad (4.15)$$

where  $V(\cdot)$  expresses speed  $u$  as a function of vehicle headways  $h$ .

Our strategy is to show that if  $T(n, x)$  is the viscosity solution of (4.14), then its partial inverse  $T(n, x)$  is the viscosity solution of (4.15). The converse will hold similarly. We begin with the definition of a viscosity solution to Hamilton-Jacobi equation of the form

$$u_t + H(\nabla u) = 0 \quad (4.16)$$

where the unknown  $u(t, x) \in \mathbb{R}^m$ ;  $\nabla u$  is the gradient of  $u$  with respect to  $x$ <sup>1</sup>. In what follows,  $C(\Omega)$  and  $C^1(\Omega)$  denote the set of continuous and continuously differentiable functions defined on  $\Omega$ , respectively.

**Definition 4.1.** A function  $u \in C(\Omega)$  is a viscosity subsolution of (4.16) if, for every  $C^1$  function  $\varphi = \varphi(t, x)$  such that  $u - \varphi$  has a local maximum at  $(t, x)$ , there holds

$$\varphi_t(t, x) + H(\nabla \varphi) \leq 0 \quad (4.17)$$

<sup>1</sup>Here  $t$  and  $x$  are dummy variables and do not necessarily represent time and space.

Similarly,  $u \in C(\Omega)$  is a viscosity supersolution of (4.16) if, for every  $C^1$  function  $\varphi = \varphi(t, x)$  such that  $u - \varphi$  has a local minimum at  $(t, x)$ , there holds

$$\varphi_t(t, x) + H(\nabla\varphi) \geq 0 \quad (4.18)$$

We say that  $u$  is a viscosity solution of (4.16) if it is both a supersolution and a subsolution in the viscosity sense.

**Remark 4.2.** If  $u$  is a  $C^1(\Omega)$  function and satisfies (4.16) at every  $x \in \Omega$ , then  $u$  is also a solution in the viscosity sense. Conversely, if  $u$  is a viscosity solution, then the equality must hold at every point  $x$  where  $u$  is differentiable. In particular, if  $u$  is Lipschitz continuous, then it is almost everywhere differentiable, hence (4.16) holds almost everywhere in  $\Omega$ .

The next theorem establishes the equivalence between viscosity solutions of (4.14) and (4.15).

**Theorem 4.3.** Assume that  $T(n, x)$  is a viscosity solution of (4.14). Furthermore, assume that  $T(n, x)$  is Lipschitz continuous in  $x$ , that is, for some  $L > 0$ ,

$$\frac{1}{v_0} |x_1 - x_2| \leq |T(n, x_1) - T(n, x_2)| \leq L |x_1 - x_2| \quad \forall x_1, x_2, \quad \forall n$$

where  $v_0$  denotes the free-flow speed. Then one can partially invert  $T(n, x)$  and get  $X(n, t)$ , which is a viscosity solution to (4.15).

*Proof.* According to our assumption,  $X(n, t)$  is strictly decreasing in  $t$  with

$$1/L |t_1 - t_2| \leq |X(n, t_1) - X(n, t_2)| \leq v_0 |t_1 - t_2| \quad \forall t_1, t_2, \quad \forall n \quad (4.19)$$

We start by showing that  $X(n, t)$  is a subsolution. Indeed, given any  $C^1$  function  $Y = Y(n, t)$  such that  $X - Y$  has a local maximum at  $(n_0, t_0)$ . Without loss of generality, we assume  $X(n_0, t_0) - Y(n_0, t_0) = 0$ . We consider the plane  $n = n_0$ , see Figure 4.

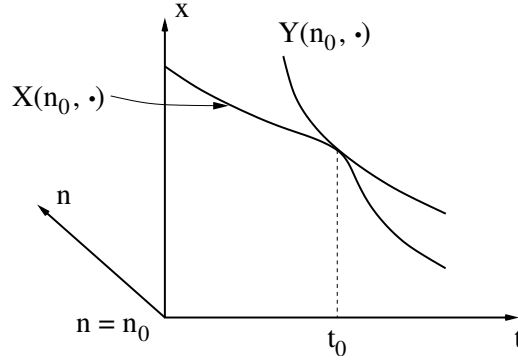


Figure 4: Graphs of  $X(n_0, \cdot)$  and  $Y(n_0, \cdot)$

Since  $X - Y$  attains a local maximum at  $(n_0, t_0)$ , by (4.19) there must hold  $Y_t(n_0, t_0) < 0$ . By continuity, there exists a neighborhood  $\Omega_1$  of  $(n_0, t_0)$  such that  $Y_t(n, t) < 0$ ,  $\forall (n, t) \in \Omega_1$ . Then we may define  $\mathcal{T}(n, \cdot)$  to be the inverse of  $Y(n, \cdot)$  in  $\Omega_1$ . Obviously,  $\mathcal{T}(n, t) \in C^1(\Omega_1)$ , and  $T - \mathcal{T}$  attains a local maximum at  $(n_0, X(n_0, t_0))$ . Using the fact that  $T(n, x)$  is a viscosity solution and applying (4.17), we deduce

$$\mathcal{T}_n(n, x) - P(\mathcal{T}_x(n, x)) \leq 0 \quad (4.20)$$

Differentiating with respect to  $n$  the identity  $Y(n, \mathcal{T}(n, x)) = x$  and using (4.20), we have

$$0 = Y_n + Y_t \mathcal{T}_n \geq Y_n + Y_t P(\mathcal{T}_x) = Y_n + Y_t P\left(\frac{1}{Y_t}\right) \quad (4.21)$$

In the above deduction, we have used the technique of differentiating both sides of  $Y(n, \mathcal{T}(n, x)) \equiv x$  with respect to  $x$  and obtaining  $1 = Y_t \cdot \mathcal{T}_x$ . Finally according to (4.21) and the monotonicity of the function  $V(\cdot)$ , we deduce

$$-Y_n \geq Y_t P\left(\frac{1}{Y_t}\right) \implies V(-Y_n) \geq V\left(Y_t P\left(\frac{1}{Y_t}\right)\right) = Y_t$$

we thus conclude that  $Y_t - V(-Y_n) \leq 0$ . Since  $Y$  is arbitrary,  $X(n, t)$  must be a subsolution. The case for supersolution is completely similar.  $\square$

## 5 Lax-Hopf Formula with Internal Boundary Conditions

When applying Lagrangian models in practical applications, the resulting boundary conditions can sometimes be irregular. One typical example is the signalized intersection in which  $u = X_t = 0$ ,  $T_x = +\infty$ . This indicates that the instantaneous travel time between vehicles are temporarily infinite, i.e. vehicles are stopped by traffic signals or the “parking lot” condition in severe congestion. In  $n$ - $x$  diagram, this case essentially creates several merged  $n$ - $x$  trajectories as illustrated in the following figure which creates irregular internal boundaries. The slope of such merged trajectories is the jam density  $k_j$  and their intersecting points with the other trajectories can be explicitly determined based on vehicle length  $L$ .

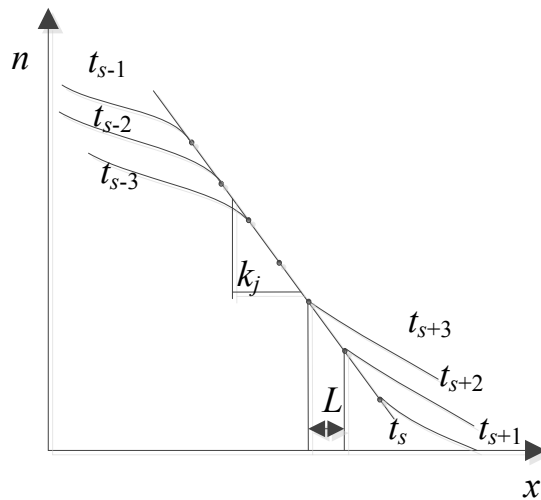


Figure 5: Illustration of the inner boundaries caused by static traffic.

Similar cases can also be found in active traffic control strategies such as variable speed limit (VSL). Traffic responding to a changing speed limit does not necessarily occur exactly at a specific location rather it occurs in a range of segment in which the VSL sign is visible. Such spatial irregularity can easily create internal boundary problems for travel time KW model. Perhaps, another type direct illustration of the internal boundary problems is the emerging

connected vehicle data sources. Vehicles with DSRC (Dedicated Short Range Communication) devices can simulatenously broadcast their locations to other vehicles or roadside sensors to be used in safety and mobility applications. When plotting such data onto the n-x diagram, we essentially obtain time trajectories. Each point in a time trajrectory represents the nth vehicle located at x location at the time of "snapshot" forming irregular internal boundaries.

In this section, we present a generalized Lax-Hopf formula for the H-J equation (4.14) with internal (irregular) boundary conditions, following the viability theory and solution representation proposed by Aubin et al. (2008). The articulation of the generalized Lax-Hopf formula requires the following definition of value conditions.

**Definition 5.1.** Given a lower-semicontinuous function  $\mathcal{D}(\cdot, \cdot)$  that maps  $\Omega$ , a subset of  $\mathbb{R}^2$ , to  $\mathbb{R}$ . The value condition  $\mathcal{C}(\cdot, \cdot)$  is defined as

$$\mathcal{C}(n, x) = \begin{cases} D(n, x) & (n, x) \in \Omega \\ +\infty & (n, x) \notin \Omega \end{cases}$$

For simplicity, let us consider a *piecewise affine* (PWA) Hamiltonian  $\mathcal{H}(\tau) \doteq -p(\tau)$  depicted in the left part of Figure 6. Define the concave transformation of the Hamiltonian:

$$\mathcal{L}(u) = \sup_{\tau \in [1/u_{free}, +\infty)} \{-p(\tau) - u\tau\} = p^* - u\tau^* \quad u \in [-w, k] \quad (5.22)$$

**Theorem 5.2. (Generalized Lax-Hopf formula)** The viability episolution to (4.14) associated with value condition  $\mathcal{C}(\cdot, \cdot)$  is given by

$$T_{\mathcal{C}}(n, x) = \inf_{(u, \tau) \in \text{Dom}(\mathcal{L}) \times \mathbb{R}_+} \{\mathcal{C}(n - \tau, x - \tau u) + \tau \mathcal{L}(u)\} \quad (5.23)$$

*Proof.* Formula (5.23) is the Lax-Hopf formula (Aubin et al., 2008) stated for the H-J equation (4.14).  $\square$

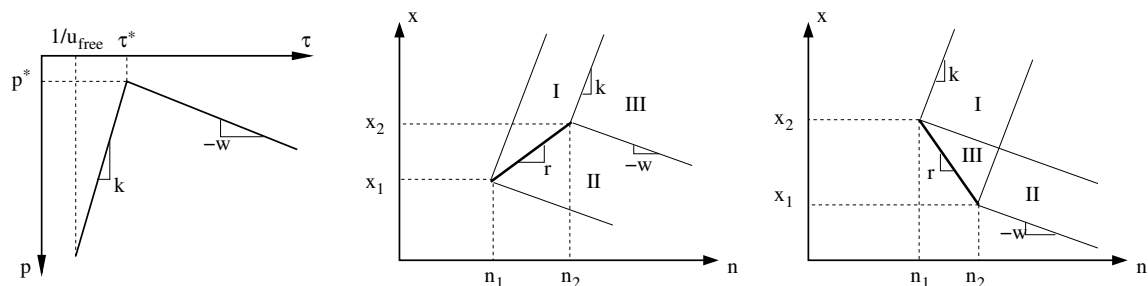


Figure 6: Left: the piecewise affine Hamiltonian. Middle: partition of the domain of dependence into three parts when  $r \in [-w, k]$ . Right: partition of the domain of dependence into three parts when  $r < -w$  or  $r > k$ .

The viability episolution in (5.23) has an important property stated below (Aubin et al., 2008)

**Proposition 5.3. (inf-morphism property)** Let  $\mathcal{C}(\cdot, \cdot)$  be the minimum of finitely many value conditions,

$$\mathcal{C}(n, x) \doteq \min_{i=1, \dots, m} \mathcal{C}_i(n, x)$$

Then

$$T_{\mathcal{C}}(n, x) = \min_{i=1, \dots, m} T_{\mathcal{C}_i}(n, x) \quad (5.24)$$

The inf-morphism property allows the H-J equation with multiple complex value conditions to be decomposed into several problems each with a single value condition. Such property tremendously simplifies solution representation and computation.

## 5.1 Piecewise Affine Internal Boundary Conditions

We consider piecewise affine (PWA) internal boundary conditions and note that any internal boundary condition with irregular domain can be approximated by PWA conditions. Per our previous discussion on the inf-morphism property, it suffices to state the Lax-Hopf formula for the simplest internal value conditions, that is, the affine ones. Piecewise affine and more complex conditions can be handled by taking the lower envelop of solutions with simple affine value conditions.

**Theorem 5.4. (Lax-Hopf formula for affine internal boundary condition)** *Given real numbers  $x_1, x_2, n_1, n_2$ , assume that the domain of the affine internal condition  $\Omega$  is a line segment with end points  $(n_1, x_1)$  and  $(n_2, x_2)$ . Let  $r = (x_1 - x_2)/(n_1 - n_2)$ . In addition, assume that the affine internal condition satisfies*

$$\mathcal{C}_{int}(n, x) = \beta + \alpha(n - n_1) \quad (n, x) \in \Omega \quad (5.25)$$

With the piecewise affine Hamiltonian depicted in Figure 6, the generalized Lax-Hopf formula (5.23) can be instantiated as follows.

(1). If  $r \in [-w, k]$ ,

$$T_{int}(n, x) = \begin{cases} \left. \begin{aligned} &\beta + \alpha \left( \frac{x_1 - n_1 r - x + nk}{k - r} - n_1 \right) + \frac{-x_1 + n_1 r + x - nr}{k - r} (p^* - k\tau^*) \\ &x - x_2 \geq k(n - n_2), \\ \text{if } &x - x_1 \leq k(n - n_1), \\ &x - x_1 \geq r(n - n_1). \end{aligned} \right\} \text{Region I} \\ \\ \left. \begin{aligned} &\beta + \alpha \left( \frac{x - x_1 + rn_1 + wn}{r + w} - n_1 \right) + \frac{-x + x_1 - rn_1 + nr}{r + w} (p^* + w\tau^*) \\ &x - x_2 \leq -w(n - n_2), \\ \text{if } &x - x_1 \geq -w(n - n_1), \\ &x - x_1 < r(n - n_1). \end{aligned} \right\} \text{Region II} \\ \\ \left. \begin{aligned} &\beta + \alpha(n_2 - n_1) + (n - n_2) \left( p^* - \frac{x - x_2}{n - n_2} \tau^* \right) \\ \text{if } &x - x_2 < k(n - n_2), \\ &x - x_2 > -w(n - n_2). \end{aligned} \right\} \text{Region III} \end{cases} \quad (5.26)$$

(2). If  $r < -w$  or  $r > k$ ,

$$T_{int}(n, x) = \begin{cases} A & \text{if } \left. \begin{array}{l} x - x_2 \leq k(n - n_2), \\ x - x_1 \geq k(n - n_1), \\ x - x_2 \geq -w(n - n_2). \end{array} \right\} \text{Region I} \\ B & \text{if } \left. \begin{array}{l} x - x_2 \leq -w(n - n_2), \\ x - x_1 \geq -w(n - n_1), \\ x - x_1 \leq k(n - n_1). \end{array} \right\} \text{Region II} \\ \min\{A, B\} & \text{if } \left. \begin{array}{l} x - x_2 < -w(n - n_2), \\ x - x_1 > k(n - n_1), \\ x - x_2 \geq r(n - n_2). \end{array} \right\} \text{Region III} \end{cases} \quad (5.27)$$

where

$$A \doteq \beta + \alpha \left( \frac{kn - x - rn_2 + x_2}{k - r} - n_1 \right) + \frac{x + rn_2 - x_2 - nr}{k - r} (p^* - k\tau^*) \quad (5.28)$$

$$B \doteq \beta + \alpha \left( \frac{wn + x + rn_2 - x_2}{r + w} - n_1 \right) + \frac{rn - x - rn_2 + x_2}{r + w} (p^* + w\tau^*) \quad (5.29)$$

*Proof.* In either case (1) or case (2), the domain of dependence can be partitioned into three disjoint regions I, II and III according to the admissible wave speeds  $k$  and  $-w$ , see the middle and right parts of Figure 6 for an illustration. Notice that in both cases, the minimum-cost path for region I is a line segment with slope  $k$ ; while the minimum-cost path for region II is a line segment with slope  $-w$ . In region III of case (1), the minimum-cost path is the segment connecting  $(n, x)$  and  $(n_2, x_2)$ ; in region III of case (2), the minimum-cost path is determined by comparing two line segments with slopes  $k$  and  $-w$ . With the above observation, simply applying (5.23) with concave transformation (5.22) yields the desired result (5.26)-(5.27).  $\square$

## 6 Difficulties in Vehicle Sinks, Sources, and Lane-Based Applications

Source term in the travel time KW model can be easily tied to the source terms in the other two representations of LWR model.

**Proposition 6.1.** *Assuming vehicle sinks and sources occur, then a source term will be attached to the RHS of each first-order conservation formulation as the following.*

$$k_t + q_x = g_V(t, x) \quad (6.30)$$

$$u_n + h_t = g_S(n, t) \quad (6.31)$$

$$\tau_n - p_x = g_T(n, x) \quad (6.32)$$

where  $g_v(t, x)$ ,  $g_s(n, t)$ , and  $g_t(n, x)$  are source terms for  $x$ - $t$ ,  $n$ - $t$ , and  $n$ - $x$  formulation respectively.

Then these source terms satisfy the following conditions.

$$g_V = -k^2 g_S = q^2 g_T \quad (6.33)$$

$$g_S = -h^2 g_V = -u^2 g_T \quad (6.34)$$

$$g_T = -\tau^2 g_S = p^2 g_V \quad (6.35)$$

*Proof.*

$$g_V(t, n) = k_t + k_n q - k q_n = -\frac{1}{h^2} (h_t + (qh)_n) = -k^2 (h_t + u_n) = -k^2 g_S(t, n) \quad (6.36)$$

Similarly,  $g_V$  can be converted to Space-Lagrangian coordinate system.

$$g_V(n, x) = q k_n + q_x + q_n (-k) = -\frac{1}{p^2} (p_x - (pk)_n) = -q^2 (p_x - \tau_n) - q^2 g_T(n, x) \quad (6.37)$$

The above two equations will lead to the rest of the equalities.  $\square$

The relationship between  $g_S$  and  $g_V$  has been proved in (van Wageningen-Kessels et al., 2013) to study the formulation and effective numerical methods to spatial conservation formulation with source terms. However, the key difficulties lie in the definition of Lagrangian coordinate itself. In mathematics, Lagrangian formulations are well-known for their difficulties in describing processes that involves breaking and merging Lagrangian systems. A typical example is tracking the water front fluctuations of lake with islands emerging and submerging at different water levels. Although the vehicle sinks and sources can be incorporated into the RHS of the PDE of Lagrangian traffic flow models, the discontinuities in the Lagrangian coordinate itself still exist. Hence, any numerical process of the Lagrangian traffic flow models need to restart every time vehicle sinks and sources occur creating new boundary problems. The travel time KW model experience less impact that the n-t Lagrangian model due to its inclusion of the spatial coordinates. In the case of n-t model, the discontinuity will result in internal boundary problems that need to be addressed either by heuristic boundary generation methods (van Wageningen-Kessels et al., 2013) or Lax-Hopf methods. The impact on the travel time KW model is primarily on the flow synchronization due to the lack of time coordinate. Both Lagrangian models will have difficulty formulating lane-by-lane traffic flow dynamics in applications such as the merging, diverging, and weaving section operations and dynamic lane control systems despite their ability to track individual vehicles.

## 7 Numerical Experiment

### 7.1 Numerical experiment and the implications to probe vehicle technologies

To illustrate the traffic flow phenomenon described by the first-order conservation law system, the NGSIM (Next Generation SIMulation) freeway trajectory data are used to show shock waves observed at the three different coordinate systems. The trajectory data is collected at eastbound I-80 in the San Francisco Bay area in Emeryville, CA, on April 13, 2005. Only trajectories over a closed section (without on/off ramps) on the I-80 corridor are chosen. Vehicles from all six lanes are used to generate the vehicular coordinates. Fundamental diagrams for each conservation law are generated based on the actual data. Detailed descriptions of these initial value problems (IVP) can be found in the following table.

No.	Conservation Law	Solution Variable	Fundamental Diagram	Initial Condition	Boundary Conditions
1	Vehicular	$k$	$q = q(k)$	$k(x, t = 0)$	$q(x_1, t)$ $q(x_2, t)$
2	Spatial	$h$	$h = h(u)$	$h(n, t = 0)$	$u(n_1, t)$ $u(n_2, t)$
3	Temporal	$\tau$	$p = p(\tau)$	$\tau(x, n = 0)$	$p(x_1, n)$ $p(x_2, n)$

Table 1: Initial-value problem defined for each conservation law.

The three IVPs in this experiment in fact reflect three different traffic monitoring configurations that can be found in practice. IVP1 represents typical fixed-point detection systems (e.g. loop detectors), in which boundary conditions (flow) can be generated continuously, while the initial conditions have to be generated by either interpolation or by a different technology such as GPS probe. IVP2 illustrates the configuration of a snapshot detection system (e.g. video detection). The continuous boundary conditions are the trajectories of two GPS probe vehicles. The initial condition is the initial spacing distribution of vehicles between those two probe vehicles. IVP3 shows a typical paired detection system, in which the boundary conditions are the continuous measures of time headways of vehicles passing two detector stations, with the initial condition as the full trajectory of a vehicle when travelling between the two detectors. The experimental results first indicate that the same traffic phenomenon can be observed in all three perspectives. The numerical results show traffic flow dynamics can be observed and measured in all three perspectives. The limitations of the first-order formulations are also clearly presented in the results. These formulations cannot capture phenomenon such as the decay of congestion if no intermediate conditions are given.

## 8 Conclusion and future work

This paper provides an in-depth discussion on the theoretical and practical aspects of applying travel time KW model in real-world traveler information and traffic management applications. The physical meaning of the travel time KW model is presented based on a heuristic derivation and a Hamilton-Jacobi theory based equivalence proof. A generalized Lax-Hopf formulation is proposed to address the internal boundary issues that may occur in field applications. Discussion and results from this paper can provide both researchers and practitioners with realistic pictures of the potentials and limitations of Lagrangian traffic flow models.

## References

- Aubin, J.P., Bayen, A.M., Saint-Pierre, P., 2008. Dirichlet problems for some Hamilton-Jacobi equations with inequality constraints. *SIAM Journal on Control and Optimization* 47(5), 2348-2380.
- Banks, J.H., 1990. Flow processes at a freeway bottleneck. *Transportation Research Record* 1287, 20-28.
- Banks, J.H., 1991. Two-capacity phenomenon at freeway bottlenecks: a basis for ramp metering? *Transportation Research Record* 1320, 83-90.

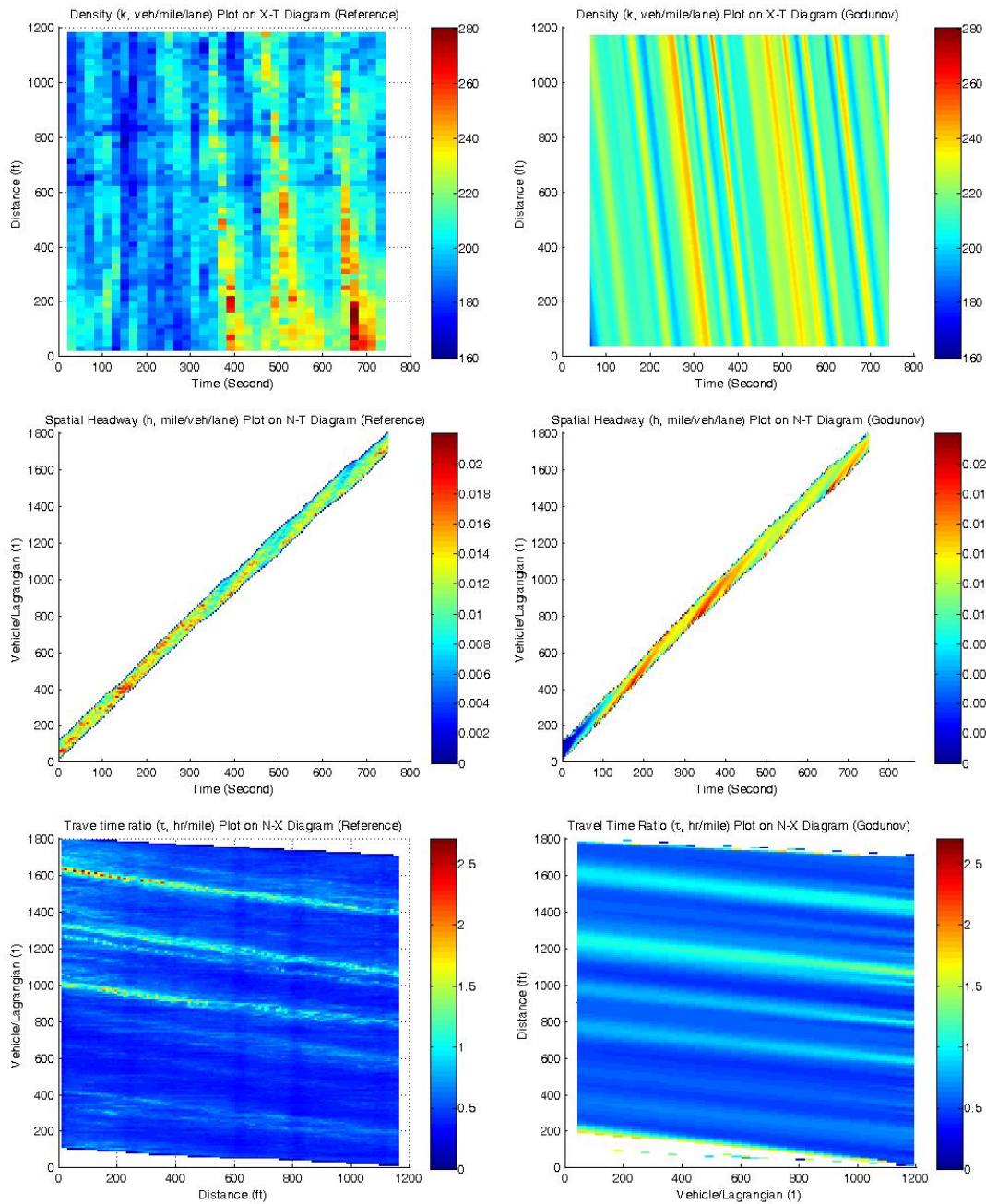


Figure 7: Numerical experimental results using Godunov schemes.

- Cassidy, M.J., Windover, J.R., 1995. Methodology for assessing dynamics of freeway traffic flow. *Transportation Research Record* 1484, 73-79.
- Cassidy, M.J., Bertini, R.L., 1999. Some traffic features at freeway bottlenecks. *Transportation Research Part B: Methodological* 33, 25-42.
- Claudel, C.G., Bayen, A.M., 2010a. Lax-Hopf Based Incorporation of Internal Boundary Conditions Into Hamilton-Jacobi Equation. Part I: Theory. *Automatic Control, IEEE Transactions on* 55, 1142-1157.
- Claudel, C.G., Bayen, A.M., 2010b. Lax-Hopf Based Incorporation of Internal Boundary Conditions Into Hamilton-Jacobi Equation. Part II: Computational Methods. *Automatic Control, IEEE Transactions on* 55, 1158-1174.
- Courant, R., Friedrichs, K., Lewy, H., 1967. On the partial difference equations of mathematical physics. *IBM Journal of Research and Development* 11, 215-234.
- Daganzo, C.F., 1994. The cell transmission model: A dynamic representation of highway traffic consistent with the hydrodynamic theory. *Transportation Research Part B: Methodological* 28, 269-287.
- Daganzo, C.F., 2005a. A variational formulation of kinematic waves: basic theory and complex boundary conditions. *Transportation Research Part B: Methodological* 39, 187-196.
- Daganzo, C.F., 2005b. A variational formulation of kinematic waves: Solution methods. *Transportation Research Part B: Methodological* 39, 934-950.
- Hall, F.L., 2001. Chapter 2 Traffic stream characteristics, *Traffic Flow Theory: A State-of-the-Art Report*. Organized by the Committee on Traffic Flow Theory and Characteristics (AHB45).
- Herrera, J.C., Bayen, A.M., 2010. Incorporation of Lagrangian measurements in freeway traffic state estimation. *Transportation Research Part B: Methodological* 44, 460-481.
- Jia, Z., Chen, C., Coifman, B., Varaiya, P., 2001. The PeMS algorithms for accurate, real-time estimates of g-factors and speeds from single-loop detectors, *Intelligent Transportation Systems, 2001. Proceedings. 2001 IEEE*. IEEE, pp. 536-541.
- Laval, J., Leclercq, L., 2013. The Hamilton-Jacobi partial differential equation and the three representations of traffic flow. *Transportation Research Part B: Methodological* 52, 17-30.
- Leclercq, L., Laval, J., Chevallier, E., 2007. The Lagrangian coordinate system and what it means for first order traffic flow models, in: Allsop, R.E., Bell, M.G.H., Heydecker, B.G. (Eds.), *17th International Symposium on Transportation and Traffic Theory (ISTTT)*. Elsevier Science, London, UK, pp. 735-753.
- Lighthill, M.J., Whitham, G.B., 1955. On kinematic waves. I. Flood movement in long rivers. II. A theory of traffic flow on long crowded roads. *Proceedings of the Royal Society of London. Series A. Mathematical and Physical Sciences* 229, 281-345.
- Luke, J.C., 1972. Mathematical Models for Landform Evolution. *J. Geophys. Res.* 77, 2460-2464.

- Makigami, Y., Newell, G.F., Rothery, R., 1971. Three-Dimensional Representation of Traffic Flow. *Transportation Science* 5, 302-313.
- Moskowitz, K., 1965. Discussion on "freeway level of service as influenced by volume and capacity characteristics" by D. R. Drew and C. J. Keese. *Highway Research Record* 99, 43-44.
- Moutari, S., Rascle, M., 2007. A Hybrid Lagrangian Model Based on the Aw-Rascle Traffic Flow Model. *SIAM Journal on Applied Mathematics* 68, 413-436.
- Newell, G.F., 1993a. A simplified theory of kinematic waves in highway traffic, part I: General theory. *Transportation Research Part B: Methodological* 27, 281-287.
- Newell, G.F., 1993b. A simplified theory of kinematic waves in highway traffic, part II: Queuing at freeway bottlenecks. *Transportation Research Part B: Methodological* 27, 289-303.
- Newell, G.F., 1993c. A simplified theory of kinematic waves in highway traffic, part III: Multi-destination flows. *Transportation Research Part B: Methodological* 27, 305-313.
- Richards, P.I., 1956. Shock waves on the highway. *Operations research* 4, 42-51.
- van Wageningen-Kessels, F., van Lint, H., Hoogendoorn, S., Vuik, K., 2010. Lagrangian Formulation of Multiclass Kinematic Wave Model. *Transportation Research Record: Journal of the Transportation Research Board* 2188, 29-36.
- van Wageningen-Kessels, F., Yuan, Y., Hoogendoorn, S.P., van Lint, H., Vuik, K., 2013. Discontinuities in the Lagrangian formulation of the kinematic wave model. *Transportation Research Part C: Emerging Technologies*.
- Wagner, D.H., 1987. Equivalence of the Euler and Lagrangian equations of gas dynamics for weak solutions. *Journal of Differential Equations* 68, 118-136.